MTA-cooperative PRMT5 inhibitors selectively modulate RNA splicing in MTAP-deleted cancer cells across histologies

Matthew R Tonini[1,2,3], Samuel Meier[1], Shangtao Liu[1], Kevin M Cottrell[1], John P Maxwell[1], Jannik Andersen[1], Alan Huang[1], Luisa Cimmino[2,3], and Kimberly J Briggs[1]

1 Tango Therapeutics, Boston, MA, USA

2 University of Miami, Miller School of Medicine, Department of Biochemistry and Molecular Biology, Miami, FL 33136, USA.

3 Sylvester Comprehensive Cancer Center, University of Miami, Miller School of Medicine, Miami, FL 33136, USA.

Abstract #

ABSTRACT

PRMT5 is a type II arginine methyltransferase that forms an active complex with methylosome protein 50 (MEP50) to catalyze the symmetric dimethylation (SDMA) of arginine residues in proteins that regulate biological roles including apoptosis, DNA damage response and RNA processing. Some of the best characterized PRMT5 substrates are SNRPB, SNRPD1 and SNRPD3, which are necessary for the formation of the spliceosome and therefore RNA splicing fidelity. MTA-cooperative PRMT5 inhibitors, including the clinical stage inhibitors TNG908 and TNG462, have been shown in preclinical studies to selectively inhibit PRMT5 in MTAP-deleted cancer cells while sparing normal, MTAP-intact cells. Consistent with this selective, on-target mechanism, treatment with TNG908 in preclinical studies results in increased aberrant RNA splicing in MTAP-deleted cells relative to MTAP-intact cells. As MTAP loss occurs in 10-15% of all human cancer the identification of a signature of alternative splicing events may report pharmacodynamic activity of PRMT5 inhibitors and potentially predict patient response. Similar splicing alterations caused by PRMT5 inhibition were identified in preclinical MTAP-deleted cancer models representing glioblastoma, non-small cell lung cancer, and others, suggesting the events are histology-agnostic. Additionally, titration of exogenous MTA, an endogenous inhibitor of PRMT5, recapitulated the observed splicing events in preclinical MTAP-proficient cells. Similar findings were observed utilizing a pharmacological inhibitor of MTAP suggesting that the identified alternative splicing events are dependent on accumulation of MTA. Collectively, these data suggest that a PRMT5-dependent RNA splicing signature can monitor the pharmacodynamic activity of MTA-cooperative PRMT5 inhibitors in MTAP-deleted cells.

MTAP-deletion and PRMT5 are a synthetic lethal pair

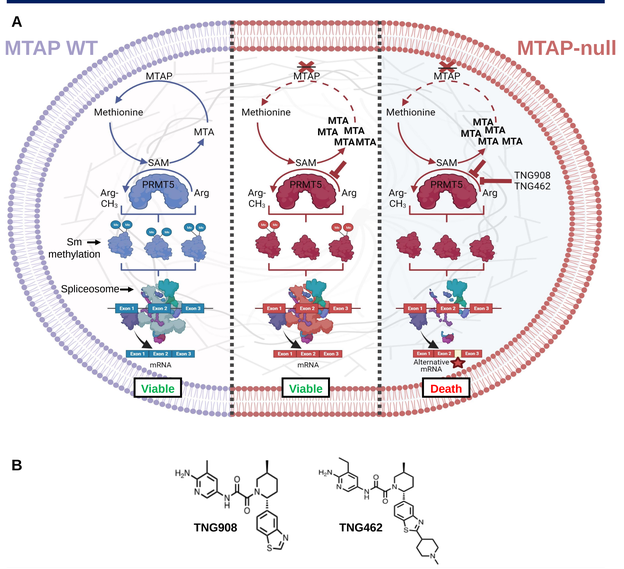

Figure 1: MTAP deletion and PRMT5 are a synthetic lethal pair. (A) Loss of MTAP, a key enzyme in the methionine salvage cycle pathway, drives the accumulation of MTA which partially inhibits the symmetric dimethylation of arginine (SDMA) residues on downstream targets. TNG908 and TNG462 are MTA-cooperative PRMT5 inhibitors that selectively inhibit PRMT5 in the presence of MTA leading to loss of cellular viability. Additionally, decreased SDMA modification of spliceosome components leads to an increase in alternative splicing of pre-mRNA transcripts (B) Chemical structures of the MTA-cooperative PRMT5 inhibitors TNG908 and TNG462.

TNG908 is selective for MTAP-deleted cancer cells

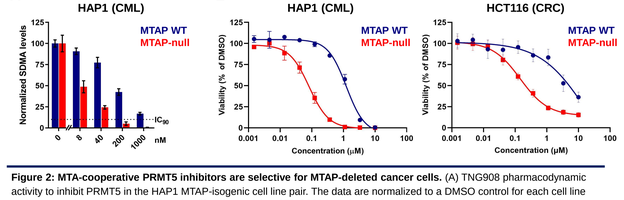

Figure 2: MTA-cooperative PRMT5 inhibitors are selective for MTAP-deleted cancer cells. (A) TNG908 pharmacodynamic activity to inhibit PRMT5 in the HAP1 MTAP-isogenic cell line pair. The data are normalized to a DMSO control for each cell line and presented as mean ± SD. (B) Antiproliferative activity of TNG908 in 7-day in vitro assays using the MTAP-isogenic cell lines HAP1 (chronic myelogenous leukemia) and HCT116 (colorectal cancer). Data are presented as mean ± SD.

TNG908 pharmacodynamic effects are histology agnostic

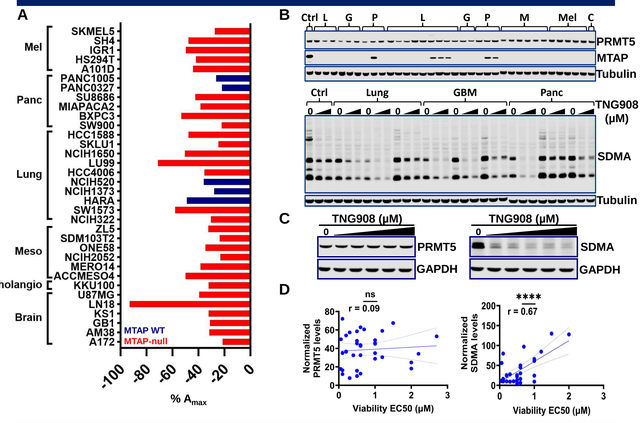

Figure 3: TNG908 pharmacodynamic effects are histology agnostic. (A) Determination of maximum effect (A_{max}) in 34 cancer cell lines representing multiple cancer lineages including melanoma, pancreatic adenocarcinoma, mesothelioma, NSCLC, cholangiocarcinoma, and glioblastoma following 7-days TNG908 treatment. Cell lines are colored by MTAP status. (B) PRMT5 and MTAP levels of cell lines from (A) (top), and exemplar SDMA immunoblot following a 3-day treatment with TNG908 at cell line-specific EC_{25} and EC_{50} concentrations. (C) PRMT5 and SDMA immunoblots following treatment a 3-day treatment of TNG908 at 0.02, 0.08, 0.31, 1.25, 5μM in MTAP-null LN18 cells. (D) Correlation of normalized PRMT5 (left) or a single SDMA-modified substrate (right) immunoblot levels at the cell line-specific EC50.

PRMT5 inhibition induces alterations in alternative splicing

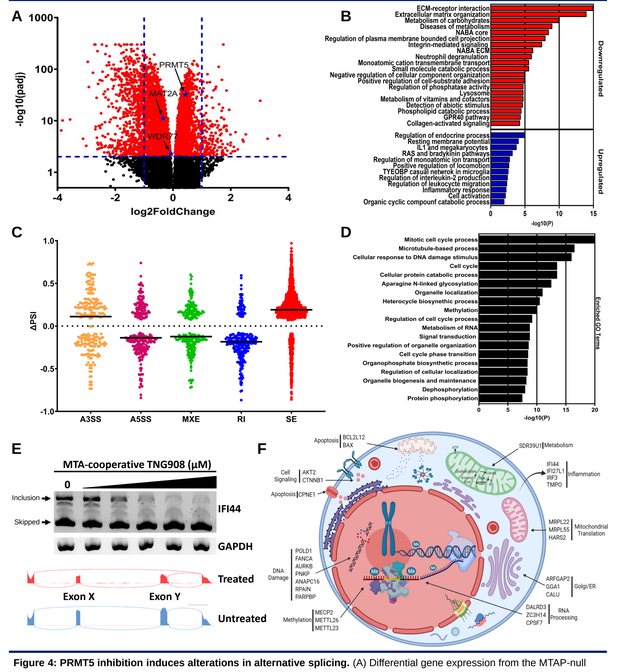

Figure 4: PRMT5 inhibition induces alterations in alternative splicing. (A) Differential gene expression from the MTAP-null GBM LN18 cell line treated for 3 days with 1μM TNG908 compared to DMSO. (B) Gene ontology analysis of significantly regulated genes from (A). (C) rMATS (replicate Multivariate Analysis of Transcript Splicing) analysis was performed on the RNAseq data from 3-day TNG908 treatment of LN18 cells to detect differential alternative RNA splicing. (D) Gene ontology analysis of skipped exons (SE) from (C). (E) Representative validation of the IFI44 SE event in LN18 cells. RT-PCR analysis to specifically detect the IFI44 exon Y skipped exon (SE) (top), and sashimi plot demonstrating ASE (below). Actual exons not labeled. TNG908 dosed at 0.001, 0.01, 0.1, 1, and 10μM. (F) Diagram demonstrating function of a subset of genes with validated alternative events.

Identified splicing alterations are dose responsive and histology agnostic

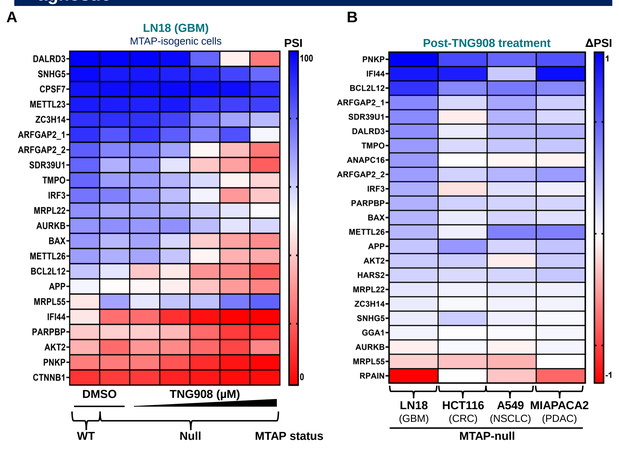

Figure 5: Validated splicing alterations are dose responsive and histology agnostic. (A) Heatmap of 22 distinct alternative splicing events (ASE) following 3-days TNG908 treatment in the MTAP-null GBM LN18 cell line. Data reported as *percent spliced in* (PSI) of the alternative exons (% inclusion = inclusion/sum of inclusion + exclusion). (B) Heatmap of 22 distinct ASEs from MTAP-null cells treated for 3 days with treated with 1μM TNG908, the maximally efficacious dose identified from Figure 2C. Data reported as ΔPSI of the alternative exons ($\Delta PSI = PSI_{DMSO} - PSI_{TNG908}$). Cell lines represent glioblastoma (GBM), colorectal cancer (CRC), non-small cell lung cancer (NSCLC), and pancreatic adenocarcinoma (PDAC).

Subset of validated events are specific for PRMT5 inhibition

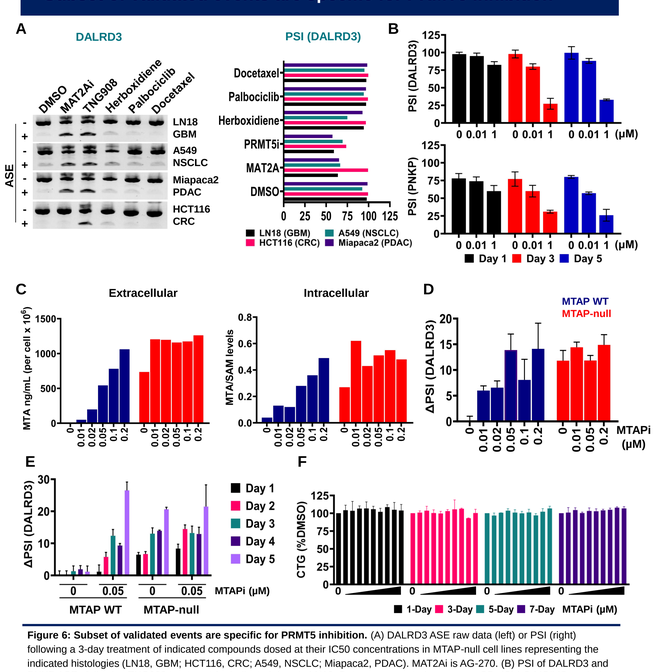

Figure 6: Subset of validated events are specific for PRMT5 inhibition. (A) DALRD3 ASE raw data (left) or PSI (right) following a 3-day treatment of indicated compounds dosed at their IC50 concentrations in MTAP-null cell lines representing the indicated histologies (LN18, GBM; HCT116, CRC; A549, NSCLC; Miapaca2, PDAC). MAT2Ai is AG-270. (B) PSI of DALRD3 and PNKP ASEs following TNG908 treatment for indicated days in LN18. Data are presented as mean ± SD. (C) LC-MS/MS analysis of MTA and SAM metabolite levels following MTAP inhibitor (MTDIA) treatment for 3 days. (D and E) ΔPSI of DALRD3 SE ($\Delta PSI = PSI_{MTAPi} - PSI_{MTAP\ WT\ DMSO}$) following MTAPi treatment at indicated doses and times in the HAP1 MTAP-isogenic cell line pair. Data are presented as mean ± SD. (F) Antiproliferative activity of MTAPi in HAP1 MTAP WT cells (10μM top dose) for indicated time points in CellTiter-Glo activity assay. Data are presented as mean ± SD.

Alternative splicing events correlate with efficacy in vitro

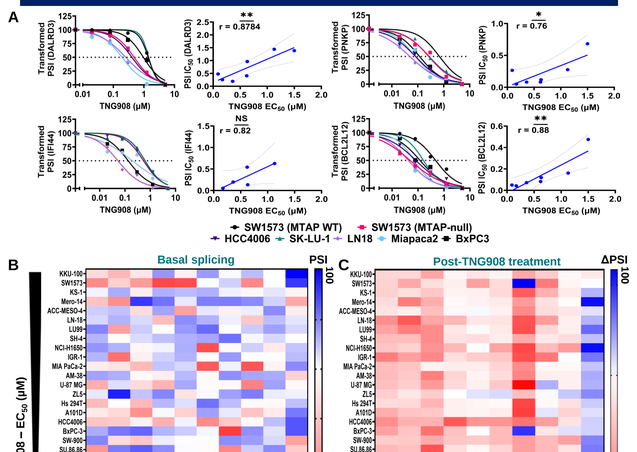

Figure 7: Alternative splicing events correlate with efficacy, but do not predict sensitivity to TNG908. (A) PSI of ASEs following 3-day TNG908 treatment in the indicated cell lines. PSI values transformed and linear regression plot was constrained at top and bottom (left). Correlation of PSI IC_{50} and viability EC_{50} (right). (B) Heatmap of basal alternative splicing in cell lines from Figure 3A ranked by sensitivity toTNG908. (C) ΔPSI of cell lines treated with TNG908 for 3 days at their specific EC_{50}.

TNG908-induced alternative splicing events occur in vivo

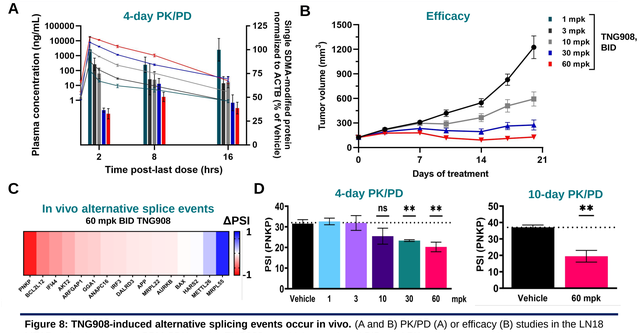

Figure 8: TNG908-induced alternative splicing events occur in vivo. (A and B) PK/PD (A) or efficacy (B) studies in the LN18 MTAP-null subcutaneous GBM CDX model. TNG908 or vehicle was dosed BID, and PK and tumor samples were collected at the indicated timepoints. N=4 tumors per group for (A), and data are presented as mean ± SEM for (A) and (B). (C) ΔPSI of the alternative exons ($\Delta PSI = PSI_{DMSO} - PSI_{TNG908}$) from tumors from (A) extracted 2-hours post last dose. (D) PSI of PNKP ASE in xenografts following TNG908 treatment for either 4 or 10 days. Data are presented as mean ± SD from 4 samples.

SUMMARY

- **TNG908 (NCT05275478) and TNG462 (NCT05732831) are actively enrolling MTAP-deleted patients in Phase 1/2 clinical trials**
- **TNG908 selectively targets *MTAP*-deleted cancer cells and induces alternative splicing events**
- **Identified alternative splicing events are PRMT5-dependent, lineage-agnostic and occur both in vitro and in vivo, but are not predictive of sensitivity to TNG908**

ACKNOWLEDGEMENTS

We thank Dr. Serge Gueroussov and Dr. Erik Wilker and the research teams at ChemPartner, WuXi and Pharmaron for their contribution to this work.